

# Vibrational-excitation cross sections of molecular oxygen by electron impact

Tong W. Shyn and Christopher J. Sweeney

*Space Physics Research Laboratory, University of Michigan, Ann Arbor, Michigan 48109-2143*

(Received 1 March 1993)

Using a crossed-beam technique, we have measured differential vibrational-excitation cross sections of the electronic ground state of molecular oxygen by electron impact. The angular range covered was from  $12^\circ$  to  $156^\circ$ , while the incident energy range of the electrons was from 5 to 15 eV. Integrated cross sections and vibrational-state energies were also obtained. The cross sections exhibit a maximum near 10 eV incident energy.

PACS number(s): 34.80.Gs

## I. INTRODUCTION

Total, elastic, and electronic excitation cross sections of molecular oxygen by electron impact have been measured by a number of researchers. Brüche [1], Sunshine, Aubrey, and Bederson [2], and Salop and Nakano [3] have measured total cross sections, while Trajmar, Cartwright, and Williams [4], Dehmel, Fineman, and Miller [5], and Shyn and Sharp [6] have measured absolute elastic differential cross sections (DCS's). For the electronic excitation cross sections, we limit our discussion to the  $a^1\Delta_g$  and  $b^1\Sigma_g$  states. Trajmar, Cartwright, and Williams [4] and Shyn and Sweeney [7] have measured differential excitation cross sections for these states.

However, while Linder and Schmidt [8] have observed vibrational excitation of molecular oxygen by electron impact, there have until the present been no measurements of the associated vibrational-excitation cross sections. Such cross sections are important to those who study the structure and dynamics of the upper atmosphere.

In this paper, we present measured differential vibrational-excitation cross sections of the electronic ground state of molecular oxygen by electron impact. A crossed-beam method was employed. The angular and incident energy ranges covered were from  $12^\circ$  to  $156^\circ$  and from 5 to 15 eV, respectively. Integrated cross sections were computed from the differential cross sections. Energies of the vibrational states were also obtained.

## II. EXPERIMENTAL APPARATUS AND PROCEDURE

The apparatus used for the present measurements was essentially the same as that used for previous measurements. As such, a detailed account of it can be found elsewhere [6,9]. Briefly, the apparatus is housed in a dual-vacuum-chamber system that is differentially pumped and contains a neutral-molecular-oxygen-beam source, a monoenergetic-electron-beam source, and an electron detection system for the scattered electrons. The vertically collimated beam of molecular oxygen is provided in the upper chamber and enters the lower chamber

via a double skimmer. The monoenergetic beam source and electron detection system are located in a horizontal plane in the lower chamber. Three sets of mutually perpendicular Helmholtz coils surround the vacuum system and reduce stray magnetic fields in the interaction region to less than 20 mG.

The electron-beam source is rotatable from  $-90^\circ$  to  $160^\circ$  continuously, and is comprised of an electron gun, a  $127^\circ$  energy selector, two electron lenses, and two beam deflectors. During the present set of measurements, it had an energy resolution of about 80 meV full width at half maximum, and produced a current of about  $10^{-9}$  A. The beam's divergence was less than  $\pm 3^\circ$ .

The detection system is fixed to the vacuum chamber wall and consists of two electrostatic analyzers in series, two electron lenses, and a Channeltron electron multiplier. This dual-analyzer system reduces the background signal by a factor of about 100 when compared to our previous single-analyzer system. The solid angle of detection afforded by our detector is about  $5 \times 10^{-4}$  sr, while its resolution is better than 60 meV.

During actual measurements, the scattering angle and

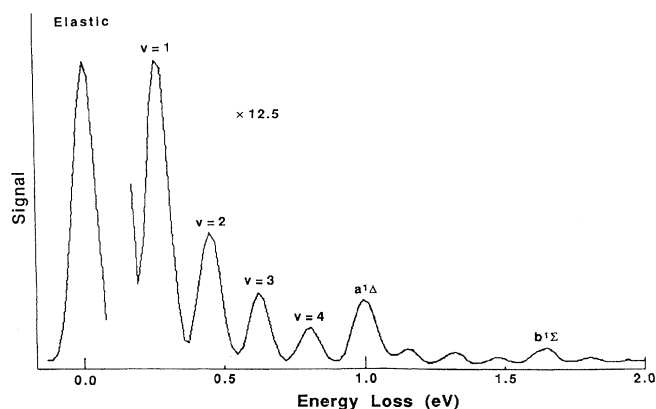


FIG. 1. Typical energy-loss spectrum for molecular oxygen. The angle and impact energy are  $96^\circ$  and 10 eV, respectively. Apparent are the first four vibrational states and the  $a^1\Delta_g$  and  $b^1\Sigma_g$  electronic states, in addition to several other states.

TABLE I. Differential vibrational-excitation cross sections of molecular oxygen. Numbers in parentheses are extrapolated data points.

$\phi$ (deg)	12	24	36	48	60	72	84	96	108	120	132	144	156	168	$\sigma_i$ ( $10^{-18}$ cm $^2$ )
$v$															
(a) $d\sigma(v)/d\Omega$ ( $10^{-19}$ cm $^2$ /sr) at 5 eV impact															
1	15	14	11	8.3	7.2	6.4	5.2	6.5	6.0	6.4	7.3	8.5	8.6	(9.0)	9.5
2	(8.2)	6.4	5.0	3.0	2.7	2.9	2.0	1.9	1.4	1.9	2.1	2.4	2.9	(3.3)	3.4
(b) $d\sigma(v)/d\Omega$ ( $10^{-19}$ cm $^2$ /sr) at 7 eV impact															
1	42	35	33	28	23	22	17	16	20	23	25	29	33	(36)	30.5
2	19	15	12	8.0	7.8	7.9	6.3	5.8	7.7	7.4	9.9	12	14	(16)	11.4
3	9.8	7.4	5.3	3.5	2.3	2.1	2.5	2.2	3.3	3.3	4.0	4.3	4.8	(5.3)	4.5
4	7.6	5.5	4.1	2.4	2.2	2.1	2.2	2.1	2.1	1.7	2.4	2.9	3.4	(3.7)	3.5
(c) $d\sigma(v)/d\Omega$ ( $10^{-19}$ cm $^2$ /sr) at 10 eV impact															
1	39	34	26	22	19	19	20	22	21	25	26	32	41	(50)	31.2
2	22	18	14	13	11	10	11	12	12	13	13	16	19	(22)	16.5
3	11	7.8	6.0	5.5	5.4	4.6	5.3	5.2	5.9	6.5	6.4	6.5	7.8	(8.5)	7.5
4	7.6	4.2	3.1	2.7	2.4	2.3	2.7	2.6	3.0	3.3	3.7	3.6	4.8	(5.3)	4.0
(d) $d\sigma(v)/d\Omega$ ( $10^{-19}$ cm $^2$ /sr) at 15 eV impact															
1	11	8.6	6.2	3.8	3.5	2.9	3.2	3.5	3.8	4.1	3.8	4.8	6.4	(8.0)	5.7
2	3.7	2.4	1.6	1.3	1.3	0.9	0.7	0.7	0.9	1.2	1.3	1.3	1.6	(1.7)	1.5
3	1.8	1.1	0.7	0.5	0.5	0.5	0.3	0.3	0.4	0.4	0.5	0.6	0.7	(0.7)	0.65
4	0.8	0.5	0.4	0.3	0.3	0.2	0.2	0.1	0.2	0.2	0.2	0.2	0.3	(0.3)	0.31

energy of the incident electrons are fixed, while the energy of the scattered electrons is swept repeatedly over the region of interest. This procedure is repeated for different scattering angles and energies. A typical energy-loss spectrum is shown in Fig. 1; it is for a scattering angle of  $96^\circ$  and an impact energy of 10 eV. Clearly visible are several vibrational states ( $v=1$  through 4) and the  $a^1\Delta_g$  and  $b^1\Sigma_g$  electronic states. Several other unidentified peaks are also present; these may represent higher-vibrational excitations of the electronic ground state, or perhaps vibrational excitations of the  $a^1\Delta_g$  and possibly  $b^1\Sigma_g$  electronic states.

In addition to cross sections, our analysis also yielded energies for the vibrational states. To within  $\pm 0.01$  eV, we have determined the energies of the  $v=1, 2, 3$ , and 4 states to be 0.19 eV, 0.39 eV, 0.57 eV, and 0.77 eV, respectively. Note that while our apparatus can resolve electronic and vibrational transitions, it is incapable of resolving rotational transitions.

Absolute values of the cross sections were obtained by normalizing to the absolute elastic cross sections measured by one of the present authors [6]. The actual procedure involved first computing the ratio between the known cross section and the measured elastic signal and then multiplying this ratio with the signal corresponding to the excitation under consideration. The impact energy scale was calibrated against the 19.3 eV resonance of helium.

### III. EXPERIMENTAL RESULTS

We have measured vibrational-excitation cross sections for the electronic ground state of molecular oxygen by a

crossed-beam technique. At an impact energy of 5 eV, the  $v=1$  and 2 cross sections were measured, while at impact energies of 7, 10, and 15 eV the  $v=1, 2, 3$ , and 4 cross sections were measured. Final results for the cross sections are given in Table I.

The statistical uncertainty in our raw data is less than  $\pm 8\%$  for 5, 7, and 15 eV, and less than  $\pm 5\%$  for 10 eV. This resulted in an overall uncertainty of less than  $\pm 17\%$  for 5, 7, and 15 eV, and less than  $\pm 15\%$  for 10 eV, when the  $\pm 14\%$  uncertainty of the elastic cross sections was accounted for.

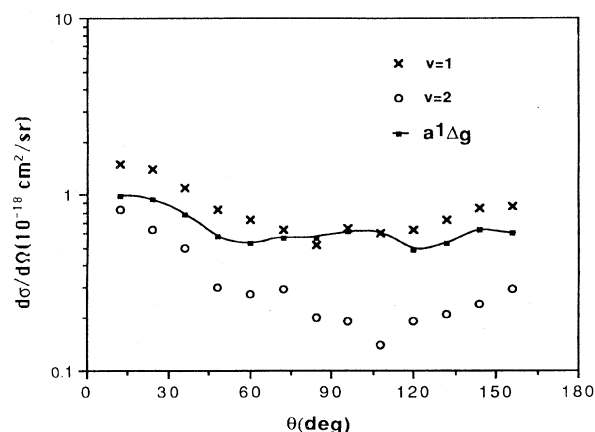


FIG. 2. Differential vibrational-excitation cross sections for  $v=1$  and 2 at 5 eV impact. Cross sections for excitation to the  $a^1\Delta_g$  state are also shown for the purpose of comparison.

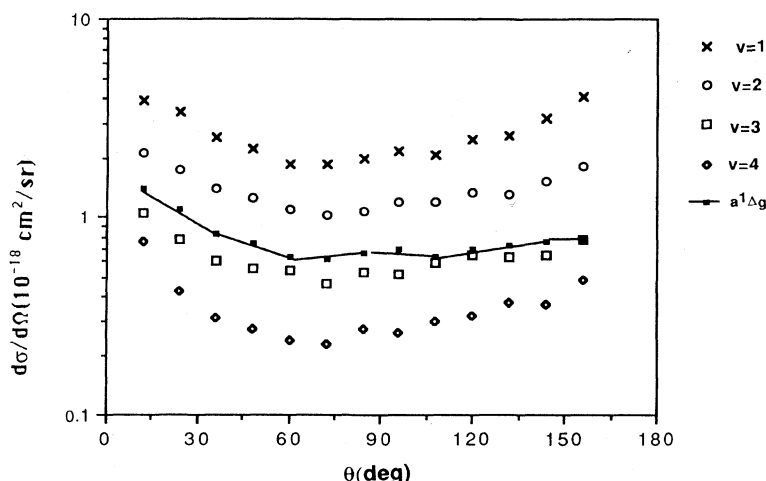


FIG. 3. Differential vibrational-excitation cross sections for  $v=1, 2, 3$ , and  $4$  at  $10$  eV impact. Cross sections for excitation to the  $a^1\Delta_g$  state are also shown for the purpose of comparison.

Figure 2 shows the angular distributions of vibrational-excitation cross sections  $v=1$  and  $2$  for  $5$  eV impact, along with  $a^1\Delta_g$  electronic-state cross sections for the purpose of comparison. The scattering is strong in the forward and backward directions, while all states have a scattering minimum near  $90^\circ$ . Note that the vibrational-excitation cross sections for  $v=1$  are larger than the  $a^1\Delta_g$  electronic-state cross sections. This same trend is apparent for the  $7$ - and  $15$ -eV results.

Figure 3 shows differential excitation cross sections for  $v=1, 2, 3$ , and  $4$  for  $10$  eV impact energy, along with the  $a^1\Delta_g$  electronic-state cross sections. Note that the  $v=1$ , and in this case also the  $v=2$ , cross sections are larger than the  $a^1\Delta_g$  electronic-state cross sections.

In Fig. 4, integrated cross sections for individual vibrational excitations are shown. A broad resonance of half-width of about  $5$  eV is apparent near  $10$  eV impact energy. Figure 5 depicts the same cross sections, but here they are plotted against the vibrational quantum number for each incident energy. Interestingly, the cross sections reduce exponentially as the quantum number increases for all incident energies. Using a least-squares technique, we have determined the best fit of this data to the function  $Ae^{-an}$ , where  $A$  is the amplitude,  $a$  the exponential decay rate, and  $n$  the vibrational quantum number.  $A$  exhibits a maximum near  $10$  eV impact energy, while  $a$  has a minimum near  $10$  eV impact. This behavior may be associated with the broad resonance and the Franck-Condon coefficients in this impact energy region.

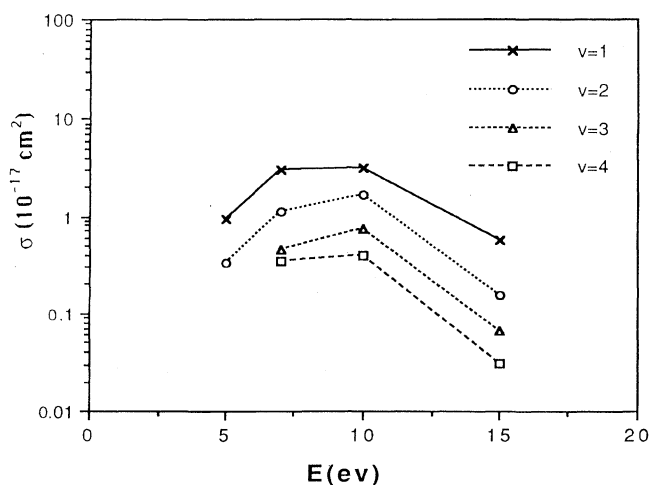


FIG. 4. Integrated vibrational cross sections vs impact energy. A maximum occurs near  $10$  eV impact energy of half-width of about  $5$  eV.

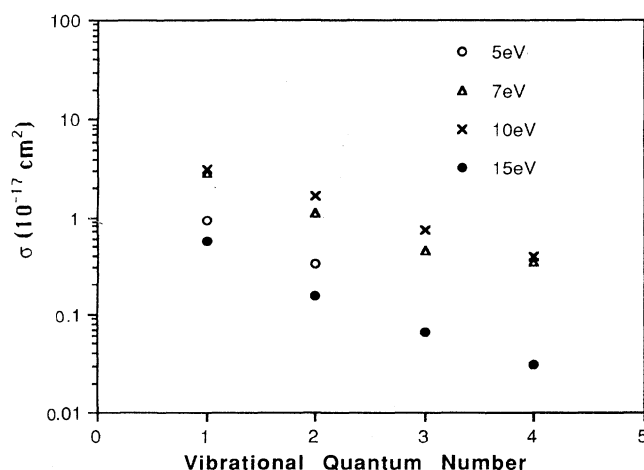


FIG. 5. Integrated vibrational cross sections vs vibrational quantum number. Note the exponential decay as the quantum number increases.

## ACKNOWLEDGMENT

This research was supported by the National Science Foundation, under Grant No. ATM-9020626.

- 
- |  |   |
|--|---|
| [1] E. Brüche, <i>Ergeb. Exakten Naturwiss.</i> <b>8</b> , 185 (1929).                         | [6] T. W. Shyn and W. E. Sharp, <i>Phys. Rev. A</i> <b>26</b> , 1369 (1982).              |
| [2] G. Sunshine, B. A. Aubrey, and B. Bederson, <i>Phys. Rev. A</i> <b>154</b> , 1 (1967).     | [7] T. W. Shyn and C. J. Sweeney, <i>Phys. Rev. A</i> <b>47</b> , 1006 (1993).            |
| [3] A. Salop and H. H. Nakano, <i>Phys. Rev. A</i> <b>2</b> , 127 (1970).                      | [8] F. Linder and H. Schmidt, <i>Z. Naturforsch.</i> <b>26</b> , 1617 (1971).             |
| [4] S. Trajmar, D. C. Cartwright, and W. Williams, <i>Phys. Rev. A</i> <b>4</b> , 1482 (1971). | [9] T. W. Shyn, S. Y. Cho, and T. E. Cravens, <i>Phys. Rev. A</i> <b>38</b> , 678 (1988). |
| [5] R. C. Dehmel, M. A. Fineman, and D. R. Miller, <i>Phys. Rev. A</i> <b>9</b> , 1564 (1974). |   |